“Fennel seeds (Foeniculum vulgare mill) Extract as Green Corrosion Inhibitor for Zinc in Hydrochloric Acid Solution”

D. M. Patel
Department of Chemistry,
C. B. Patel Computer College & J. N. M. Patel Science College,
Surat, Gujarat, India.
Email:- darshakpatel81526@gmail.com
Mo:- 7069168111

V. R. Patel
Department of Chemistry,
C. B. Patel Computer College & J. N. M. Patel Science College,
Surat, Gujarat, India.
Email:- virendrapatel1501@gmail.com
Mo:- 8849142054

B. M. Patel
Department of Chemistry,
C. B. Patel Computer College & J. N. M. Patel Science College,
Surat, Gujarat, India.
Email:- patelbhavesh5996@gmail.com
Mo:- 9687918143

S. A. Desai
Department of Chemistry,
C. B. Patel Computer College & J. N. M. Patel Science College,
Surat, Gujarat, India.
Email:- desai.sagar@hotmail.com
Mo:- 9825127809

Abstract:

Fennel seeds (Foeniculum vulgare mill) as a green corrosion inhibitor for zinc in an HCl solution have been investigated by mass loss (ML), Potentiodynamic Polarization (PDP), Electrochemical Impedance Spectroscopy (EIS), Fourier Transform Infrared Spectroscopy (FTIR), Scanning Electron Microscope (SEM), and Energy Dispersive X-ray Spectroscopy (EDX) techniques. The highest I.E. for this inhibitor was 91.92% after a 24 h immersion time at 2.5 g/L inhibitor concentration in 0.08 N HCl solution. polarization result indicating that the inhibitor act as a mixed-type inhibitor. The graph of Nyquist plots is nearly semicircular, which suggests that the charge transfer process mainly inhibits zinc corrosion. From the data obtained at various temperatures (313K, 323K, 333K), the thermodynamic parameters and kinetic parameters were calculated for the tested system. The inhibitor molecule adsorption on the zinc surface followed the Langmuir adsorption isotherm. The results showed that fennel seeds extract effectively inhibits zinc corrosion in HCl solution.

1. Introduction:

Corrosion is an irreversible electrochemical reaction in which the metal reacts with the surrounding atmosphere, resulting in the creation of a more chemically stable form such as oxide, hydroxide, sulphide, and chloride. zinc an important nonferrous metal is the fourth most used metal in the world and it has innumerable uses in industrial as well as in other segments [1]. Hydrochloric acid is widely used in industry, industrial acid cleaning, acid descaling and oil-well cleaning [2]. The use of inhibitors is one of the most practical methods for protection against corrosion. The hazardous nature, nonbiodegradability and cost of these organic compounds [3-10] motivated the researchers to focus their attention on developing cheap, nontoxic, biodegradable and environmentally friendly natural products of plant origin as corrosion inhibitors. Researchers were found some green corrosion inhibitors for zinc in HCl like as Kanchaki [11], Rosmarinus [12], Bili leaf [13], Moringa oleifera and Mangifera indica [14], Newbouldia leavis and Pepper fruit [15], Hyssopus officinalis [16] etc. In the present work, the effect of fennel seeds extract as a zinc corrosion inhibitor in hydrochloric acid has been reported in this work.

2. Experimental:

2.1 Sample and solution preparation:

The composition of zinc metal: 99.16% Zn, 0.46% Fe, 0.18% Cr, and 0.21% Ni was used in the present study. The metal specimens of size 5.5 cm x 2.0 cm x 0.14 cm having an effective area of 0.2418 dm^2 were used. The corrosion medium having concentrations of 0.08, 0.10, and 0.12 N was prepared by diluting analytical grade HCl purchased from Merck using double distilled water.

2.2 Green Inhibitor Solution preparation:

Fennel seeds extract was prepared by refluxing 10.0 gm of fennel seeds powder with 100 ml of methanol for about 30 minutes. Filtered and removed alcohol to get a yellow sticky mass, which was used to prepare the required inhibitor concentrations of 1.0, 1.5, 2.0, and 2.5 g/L of fennel seeds extract.

2.3 Mass loss measurements:

For this study, the zinc plates were completely dipped in 200 ml of 0.08, 0.10, and 0.12 N HCl solution using glass hooks to determine the corrosion rate in the absence and presence of various inhibitor concentrations at room temperature (301±1 K) for 24 h. The values of the corrosion rate were reported in mg/dm²d.

2.4 Effect of temperature:

To study the effect of temperature on corrosion of zinc in 0.10 N HCl, the specimens were immersed in 200 ml of the corrosive solution and mass loss was determined at solution temperatures of 313, 323 and 333 K for an immersion period of 2 h without and with inhibitor at various concentrations. Kinetic Parameter: Rate constant (K) and half-life (t1/2), and Thermodynamic parameter: free energy of adsorption (ΔGads), heat of adsorption (Qads), energy of activation (Ea), enthalpy of adsorption (ΔHads), and entropy of adsorption (ΔSads) were calculated at various temperatures.

2.5 Potentiodynamic Polarization (PDP) measurement:

The PDP studies were made using a potentiostat/galvanostat meter [Instruments: GAMRY - Reference 600]. In this experiment, Ag/AgCl was used as a reference electrode, platinum as an auxiliary electrode, and zinc metal was used as a working electrode. For the polarization study, zinc specimen having an area of 1 cm² were exposed to 200 ml of 0.08 N HCl with and without inhibitors. Tafel lines are drawn to the respective corrosion potentials (Ecorr) to determine the corrosion current density (Icorr) [17]. Cathodic Tafel slope (βc) and anodic Tafel slope (βa) were calculated.

2.6 Electrochemical impedance spectroscopic (EIS) measurements:

For this study, we find out using the same procedure using a potentiodynamic polarization experiment. A continuous AC voltage with a small amplitude (5.0 mV) and a broad frequency range of 1 to 100 kHz was supplied to the system. A real impedance (Z') versus imaginary impedance (Z″) graph was plotted. The double layer capacitance (Cdl) and charge transfer resistance (Rct) were calculated from the Nyquist plots. Both with and without inhibitors present, impedance measurements were performed.

2.7 Scanning Electron Microscope (SEM) measurements:

A high-energy electron beam scan was used to analyze the surface of the zinc plate. A number of signals, including secondary electrons, back-scattered electrons, absorbed

electrons, transmitted electrons, cathode luminescence, and X-rays, are emitted by the metal plate when it is exposed to a high-energy electron beam. For this technique the secondary electron signals are mainly used to take the image of the metal plate in the absence and presence of the inhibitor. For this study, zinc specimen having an area of 1 cm^2 were exposed to 200 ml of 0.08 N HCl solution with and without inhibitor at room temperature (301±1K) for 24 h.

2.8 Energy dispersive x-ray spectroscopic (EDX) measurements:

EDX spectra are used to find out the elements present on surface of the zinc plates. For this study, zinc specimen having an area of 1 cm^2 were exposed to 200 ml of 0.08 N HCl solution with and without inhibitor at room temperature (301±1K) for 24 h.

2.9 Fourier Transform Infrared Spectroscopy (FTIR):

For this study the zinc plates having an area of 1 cm^2 were completely immersed in 200 ml of 0.08 N HCl solution in the absence and presence of inhibitor at room temperature (301±1 K) for 24 h. FTIR spectra of the methanol extract from fennel seeds were recorded. FTIR spectra were recorded in an extend range between wavelengths of 400 cm-1 to 4000 cm-1.

3. Result and Discussion:

3.1 Mass loss measurements:

The corrosion rate of zinc in 0.08, 0.10, and 0.12 N HCl solutions in the absence and presence of 1.0, 1.5, 2.0, and 2.5 g/L concentrations of fennel seeds extract for an immersion period of 24 h at room temperature (301±1K) was calculated from mass loss data (Table 1) using the following equation:

Equation for corrosion rate, % Inhibition Efficiency (I.E) and surface coverage:

$$\text{corrosion rate } \left(\frac{\text{mg}}{\text{dm2d}}\right) = \frac{\text{mass loss (gm)} \times 1000}{\text{Effective surface area (dm}^2\text{)} \times \text{Time (day)}} \quad \ldots\ldots\ldots\ldots(1)$$

$$\%\ \text{I. E.} = \left(\frac{(W_u - W_i)}{W_u}\right) \times 100 \quad \ldots\ldots\ldots\ldots....(2)$$

$$\text{Surface covrage } (\theta) = \left(\frac{(W_u - W_i)}{W_u}\right) \quad \ldots\ldots\ldots\ldots....(3)$$

Where, Wu is the Mass loss of metal in acid (absence of inhibitor) and Wi is the Mass loss of metal in acid (presence of inhibitor).

3.2 Acid concentration effect:

The corrosion rate increases with the increase in concentration of acid. The corrosion rate was 2150.36, 2646.60, and 3184.19 mg/dm^2d for 0.08, 0.10, and 0.12 N hydrochloric acid concentrations, respectively, for an immersion period of 24 h at 301 K, as shown in Table 1.

3.3 Effect of inhibitor concentration:

With an increase in inhibitor concentration, the rate of corrosion decreases while I.E. increases. I.E. was found to be 67.50, 76.73, 88.46, and 91.92%, corresponding to 1.0, 1.5, 2.0, and 2.5 g/L inhibitor concentrations, respectively, in 0.08 N HCl (Table 1, Fig. 1). As acid concentration increases, the IE of fennel seeds extract decreases. I.E. was found to be 91.92, 84.22, and 81.56%, corresponding to 0.08, 0.10, and 0.12 N HCl, respectively, in 2.5 g/L inhibitor concentration (Table 1, Fig. 2).

Table 1: Effect of acid concentration on Corrosion rate (C.R.) and Inhibition Efficiency (I.E.) of zinc in HCl acid containing fennel seeds extract as an inhibitor for an immersion period of 24 h at 301 ± 1 K.

Inhibitor concentration g/L	Concentration of HCl					
	0.08 N HCl		0.10 N HCl		0.12 N HCl	
	C.R. (mg/dm²d)	%IE	C.R. (mg/dm²d)	%IE	C.R. (mg/dm²d)	%IE
Blank	2150.36	-	2646.60	-	3184.19	-
1.0	698.87	67.50	1616.91	38.91	2365.40	25.71
1.5	500.37	76.73	1029.69	61.09	1943.59	38.96
2.0	248.12	88.46	665.78	74.84	1203.37	62.21
2.5	173.68	91.92	417.67	84.22	587.21	81.56

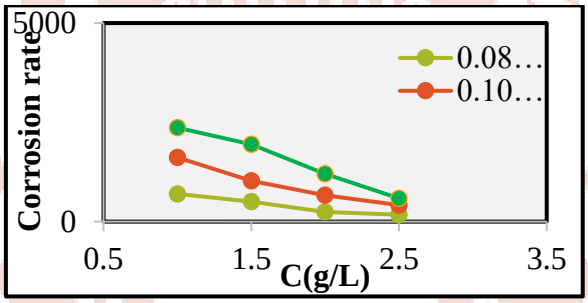

Fig. 1: Corrosion rate (C.R.) of zinc in 0.08, 0.10, and 0.12 N HCl solution in presence of different concentration fennel seeds extract for an immersion period of 24 h at 301 ± 1 K.

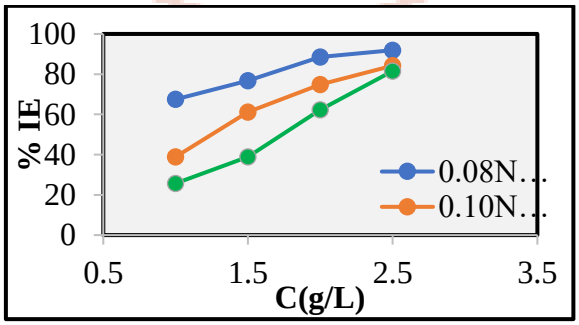

Fig. 2: Inhibition Efficiency (I.E.) of zinc in various concentrations HCl acid containing 1.0, 1.5, 2.0, and 2.5 g/L fennel seeds extract as an inhibitor for an immersion period of 24 h at 301 ± 1 K.

3.4 Effect of temperature:

To investigate the effect of temperature on corrosion of zinc in 0.10 N HCl, mass loss experiments are carried out at temperatures of 313 K, 323 K, and 333 K without and with fennel seeds extracts for an immersion period of 2 h. The corrosion rates for 0.10 N HCl were 6451.08, 7443.55, and 9924.74 mg/dm²d at temperatures 313K, 323K, and 333K, respectively.

Inhibitor concentration g/L	Concentration of HCl					
	313K		323K		333K	
	C.R. (mg/dm²d)	%IE	C.R. (mg/dm²d)	%IE	C.R. (mg/dm²d)	%IE
Blank	6451.08	-	7443.55	-	9924.74	-
1.0	744.36	88.46	1339.84	82.00	2233.07	77.50
1.5	496.24	92.31	793.98	89.33	1488.71	85.00
2.0	347.37	94.62	645.11	91.33	1091.72	89.00
2.5	148.87	97.69	396.99	94.67	1042.10	89.50

As the temperature increases, the corrosion rate increases while the percentage of I.E. decreases (Table 2). e.g., in 0.10 N HCl at 2.5 g/L inhibitor concentration, the I.E. for fennel seeds extract was 97.69, 94.67, and 89.50% at 313K, 323K, and 333K, respectively. The desorption of the adsorbed molecules at higher temperatures may be the cause of the increased corrosion loss, which opens the new metal surface to more attack [18].

3.4.1 Energy of activation (E_a):

The value of 'Ea' was calculated from the slope of log ρ versus 1/T (ρ = corrosion rate, T = absolute temperature) and also by using the Arrhenius equation [19]:

$$log\frac{\rho_2}{\rho_1} = \frac{E_a}{2.303\,R}\left[\frac{1}{T_1} - \frac{1}{T_2}\right] \qquad \text{…….(4)}$$

Were, ρ1: corrosion rate at temperature T1, ρ2: corrosion rate at temperature T2

Ea from the graph = 2.303 x R x Slope …….....(5)

Results given in Table 3 show that mean 'Ea' values were higher in inhibited acid (ranging from 47.52 to 84.34 kJmol⁻¹) than the 'Ea' value for the uninhibited system (18.87 kJmol⁻¹).

Table 3: Activation energy (E_a) and Free energy of adsorption (ΔG_{ads}) for zinc in 0.10 N HCl acid at various concentrations of fennel seeds extract for an immersion period of 2 h.

Inhibitor concentration g/L	Energy of activation (E_a) KJ/mol				Free energy of adsorption (ΔG_{ads}) KJ/mol		
	313-323K	323-333K	Mean	From Arrhenius Plot	313K	323K	333K
Blank	12.02	25.72	18.87	18.60	-	-	-
1.0	49.37	45.67	47.52	47.63	-14.83	-14.39	-14.68
1.5	39.48	56.21	47.84	47.52			
2.0	52.00	47.04	49.52	49.65			
2.5	82.38	86.29	84.34	84.31			

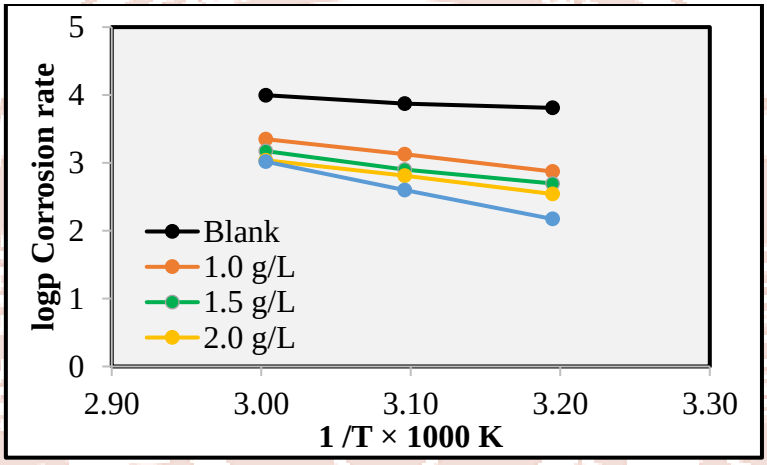

Fig. 3: Arrhenius plots for corrosion of zinc in 0.10 N HCl in absence and presence of different concentration of inhibitor extract.

3.4.2 Free energy of adsorption (ΔGads):

$\Delta Gads = - RT \ln (55.5 Kads)$ ……..…...(6)

where R is the gas constant, T is the absolute temperature, and Kads is the desorption/adsorption process' equilibrium constant [20]. The negative values of ΔGads of inhibitor (ranging from -14.39 to -14.83 kJ/mol in Table 3 indicate that the inhibitor molecules adsorption on the metal surface is a spontaneous exothermic reaction [21].

3.4.3 Heat of adsorption (Qads):

Heat of adsorption (Qads.) values were derived as follows [22],

$$Q_{ads} = -2.303\ R \left[\log\left(\frac{\theta_2}{(1-\theta_2)}\right) - \log\left(\frac{\theta_1}{(1-\theta_1)}\right)\right] \times \left[\frac{T_1 T_2}{T_2 - T_1}\right] \quad \text{……..……(7)}$$

where, θ1 and θ2 are the surfaces covered by the inhibitors on metal at temperatures T1 and T2, respectively.

The value of Qads were negative and ranged from -23.64 to -73.07 kJ/mol, indicating that the adsorption process favored the physisorption mechanism [23].

Table 4: Thermodynamic parameters: Heat of adsorption (Q_{ads}), Enthalpy of adsorption (ΔH_{ads}), and Entropy of adsorption (ΔS_{ads}) for zinc in 0.10 N HCl acid at various concentrations of fennel seeds extract for an immersion period of 2 h.

Inhibitor Conc. (g/L)	Q_{ads} (KJ/mol)		ΔH_{ads} (KJ/mol)		ΔS_{ads} (KJ/mol K)	
	313-323K	323-333K	313-323K	323-333K	313-323K	323-333K
Blank	-	-	9.38	22.99	-	-
1.0	-43.76	-25.01	46.73	42.94	0.197	0.178
1.5	-30.24	-34.94	36.84	53.48	0.165	0.210
2.0	-42.98	-23.64	49.36	44.31	0.205	0.182
2.5	-73.07	-65.61	79.74	83.56	0.302	0.303

3.4.4 Enthalpy of adsorption (ΔHads):

ΔHads was calculated using the equations (8):

$$\Delta Hads = Ea - RT \quad \text{……. (8)}$$

The difference in enthalpy (ΔHads) was positive and ranged between 42.94 to 83.56 kJ/mol suggesting the reaction is endothermic in nature and indicating that higher temperature favors the corrosion process [24].

3.4.5 Entropy of adsorption (ΔSads):

ΔSads [25] were calculated using the equations (9):

$$\Delta Sads = \Delta Hads - \Delta Gads /T \quad \text{……..(9)}$$

Positive values of ΔSads ranging from 0.165 to 0.303 kJ/mol K Suggested that the system is entropically favorable [25].

3.4.6 Kinetic parameters: The rate constant ‘k’ and Half-life (t1/2):

The rate constant ‘k’ are calculated using the following equation [26]:

$$K = \frac{1}{t} \ln\left(\frac{W_i}{W_f}\right) \quad \text{…….(10)}$$

where, Wi is the initial weight of the sample (before immersion), Wf is the final weight of the sample (after immersion) and ‘t’ is the immersion time (in days).

The values of half-life (t1/2) are using the equation below [27]:

$$t_{\frac{1}{2}} = \frac{0.693}{K} \quad \text{…….(11)}$$

where, ‘t’ is time in days and k is the rate constant.

Table 5: Kinetic parameters: Rate constant 'K' and Half-life '$t_{1/2}$' for the corrosion of zinc in 0.08, 0.10 and 0.12 N concentration of HCl containing various concentration of fennel seeds extract.

Inhibitor concentration g/L	Concentration of HCl					
	0.08 N HCl		0.10 N HCl		0.12 N HCl	
	Rate constant	Half-life	Rate constant	Half-life	Rate constant	Half-life
Blank	48.65	14.24	61.68	11.24	74.91	9.25
1.0	15.77	43.93	36.87	18.79	53.91	12.86
1.5	11.32	61.24	23.61	29.36	44.16	15.69
2.0	5.63	123.10	15.15	45.74	27.48	25.22
2.5	3.89	178.23	9.40	73.75	13.23	52.38

As the concentration of the inhibitor increases, the half-life increases, whereas the rate constant k decreases. Concentration of acid increases Corrosion rate constant "K" also increases.

3.5 Adsorption isotherm:

The Langmuir isotherm is given by the following equation [28]:

$$\frac{C}{\theta} = \frac{1}{K_{ads}} + C \qquad \ldots\ldots\ldots\ldots(12)$$

Where C is the concentration of inhibitor, Kads is the equilibrium constant of the adsorption process, and θ is the surface coverage.

Plot C/θ versus C yields showed a straight line indicating that the inhibitor followed the Langmuir adsorption isotherm.

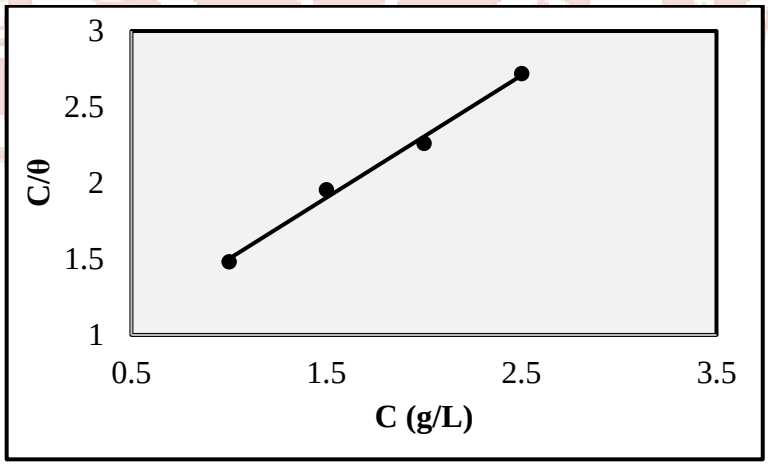

Fig. 4: Langmuir adsorption isotherm for zinc in 0.08 N HCl acid.

3.6 Potentiodynamic Polarization measurements:

Electrochemical parameters such as corrosion current density (icorr), corrosion potential (Ecorr) and percentage of I.E. were given in Table 6. Polarization curves for zinc in 0.08 N HCl in the absence and presence of 2.5 g/L fennel seeds extract were shown in Fig. 5a and Fig. 5b.

Inhibition efficiency (I.E.) from the polarization study was calculated using the following equation:

$$\text{I. E. (\%)} = \frac{i_{corr(uninh)} - i_{corr(inh)}}{i_{corr(uninh)}} \times 100 \qquad \text{.....(13)}$$

Where icorr (uninh) indicates corrosion current density in uninhibited acid, whereas icorr (inh) indicates corrosion current density in inhibited acid.

The polarization curves show polarization of both the anodes and the cathodes. Usually, if the variation Ecorr compared to the blank is more than 85 mV, the inhibitor is either cathodic or anodic [29]. In this study, the maximum variation of Ecorr for the inhibitors was 15 mV (Table 6), which indicates that the inhibitors work as mixed-type inhibitors. I.E. from Tafel plots were in good agreement with the I.E. obtained from weight loss data.

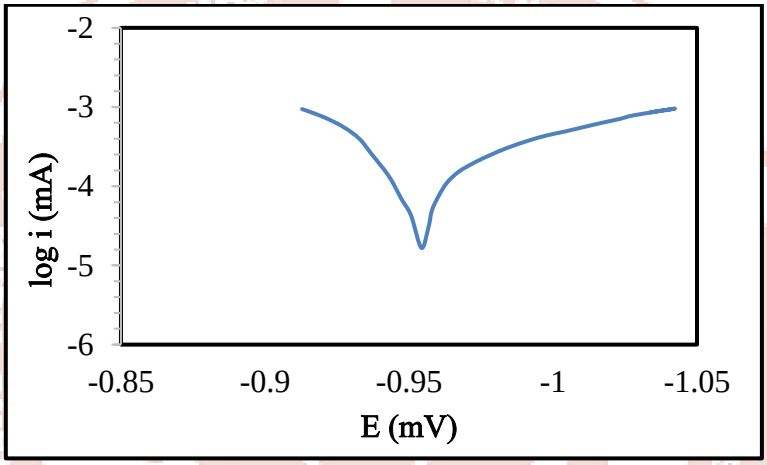

Fig. 5a: Polarisation curve for corrosion of zinc in 0.08 N HCl.

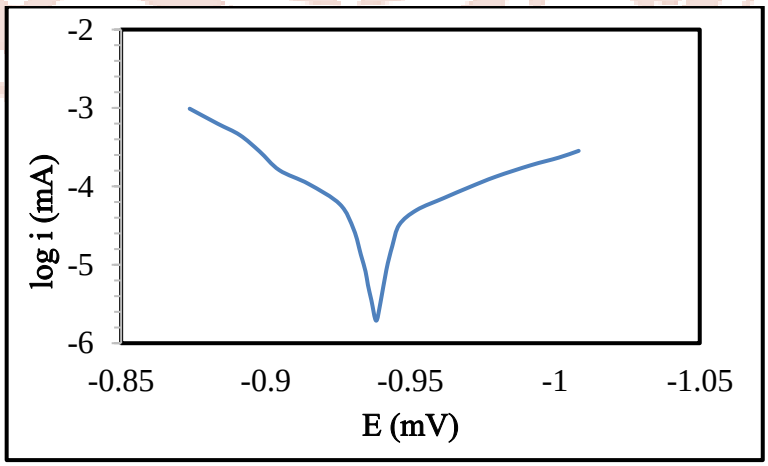

Fig. 5b: Polarisation curve for corrosion of zinc in 0.08 N HCl containing at 2.5 g/L inhibitor concentration.

Table 6: Polarization data and inhibition efficiency (I.E.) of fennel seeds extract for Zinc in 0.08 N HCl acid at 2.5 g/L inhibitor concentration.

System	E_{corr} (mV)	I_{corr} ($\mu A/cm^2$)	Tafel slope (mV/decade)		Tafel Constant B (mV)	By Weight Loss method	By Polarization method
			+βa	-βc			
Blank	-954	209.60	62.7	118.0	17.80	-	-
Fennel seeds extract	-939	30.13	47.6	63.5	11.83	91.92 %	85.63 %

3.7 Electrochemical impedance spectroscopic (EIS) measurements:

EIS is a helpful technique for analyzing how a metal surface interacts and estimating the rate at which it may corrode. As shown in Fig. 6a and Fig. 6b, Nyquist plots for zinc corrosion in a 0.08 N HCl solution with and without an inhibitor were analyzed using the EIS study.

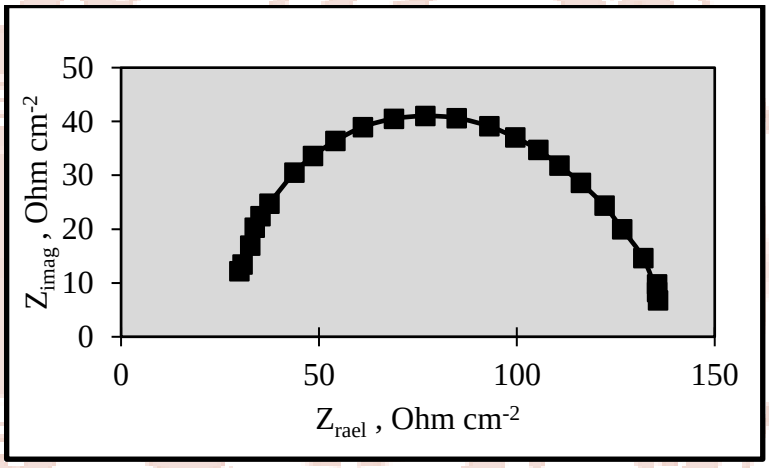

Fig. 6a: Nyquist plots for corrosion of zinc in 0.08 N HCl.

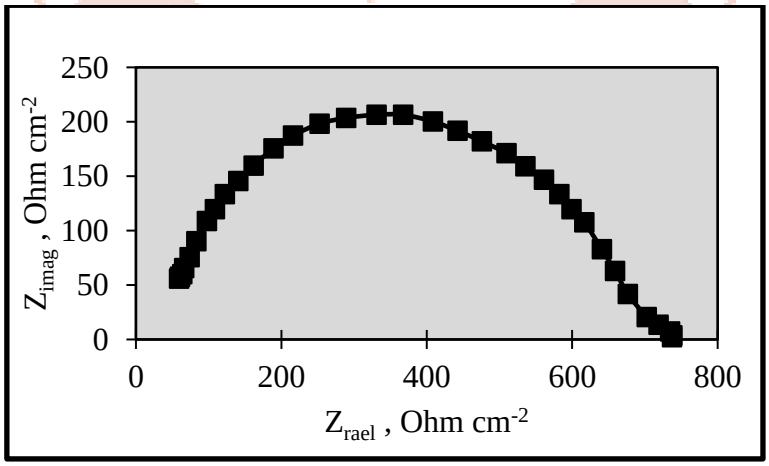

Fig. 6b: Polarisation curv Nyquist plots for corrosion of zinc in 0.08 N HCl containing at 2.5 g/L inhibitor concentration.

Table 7 presents the EIS results. The capacitive circle width is higher when the inhibitor is present than when it is absence. R_{ct} is related to the high-frequency capacitive loop. To calculate C_{dl}, the frequency at which the imaginary component of the impedance is maximum was found as inhibition efficiency (I.E.) from the EIS method was calculated using the following equation [30]:

$$I.E.(\%) = \frac{C_{dl(uninh)} - C_{dl(inh)}}{C_{dl(uninh)}} \times 100 \qquad \text{.....(14)}$$

Where i_{corr} (uninh) indicates corrosion current density in uninhibited acid whereas. i_{corr} (inh) indicates corrosion current density in inhibited acid.

Table 7: EIS parameters and inhibition efficiency (I.E.) of fennel seeds extract for Zinc in 0.08 N HCl acid at 2.5 g/L inhibitor concentration.

System	R_{ct} (Ohm / cm^2)	Cdl (µF/cm^2)	By Weight Loss method	By EIS method
Blank	135.66	179.67	-	-
Feenel seed Extract	737.64	6.57	91.92 %	96.35 %

The inhibitor addition increases R_{ct} values from 135.66 to 737.64 Ω cm^2, and decreases the C_{dl} values from 179.67 to 6.57 µF/cm^2, which is due to the inhibitor adsorption onto the metal surface.

3.8 Scanning Electron Microscope (SEM) measurements:

SEM images were acquired to understand the metal specimens' surface condition with and without the inhibitor. Fig. 7 represents the SEM images.

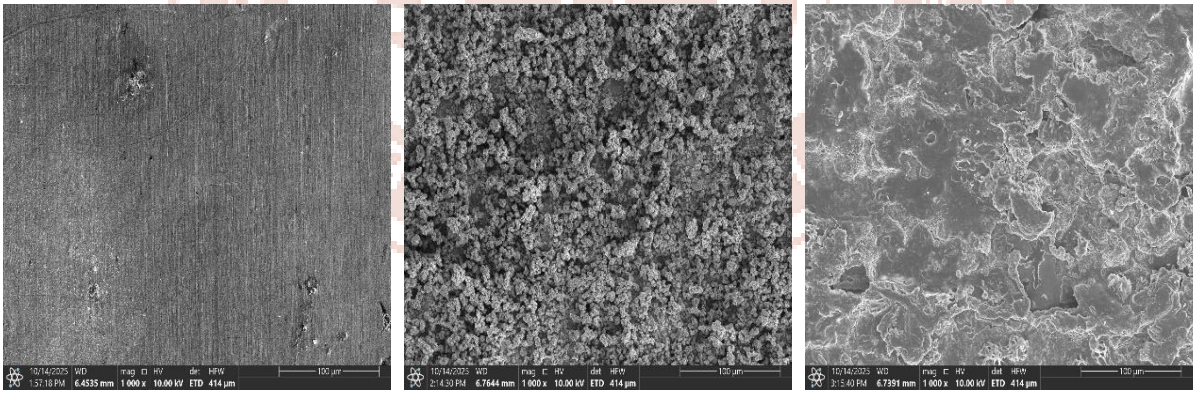

(7a) **(7b)** **(7c)**

Fig. 7: Zinc surface SEM images: (7a) polished zinc, (7b) zinc immersed in 0.08 N HCl and (7c) zinc immersed in 0.08 N HCl with 2.5 g/L fennel seeds extract.

A smooth surface is seen in the SEM image of the previously polished zinc (Fig. 7a), whereas the heterogeneous surface of zinc with large pits in the 0.08 N HCl media (Fig. 7b) suggests the metal faced pitting corrosion in the HCl medium. [31]. On the other hand, the zinc

SEM image in the presence of 2.5 g/L inhibitor extract in the 0.08 N HCl solution (Fig. 7c) showed an increase in surface smoothness compared to the absence of inhibitor.

3.9 Energy dispersive x-ray spectroscopic (EDX) measurements:

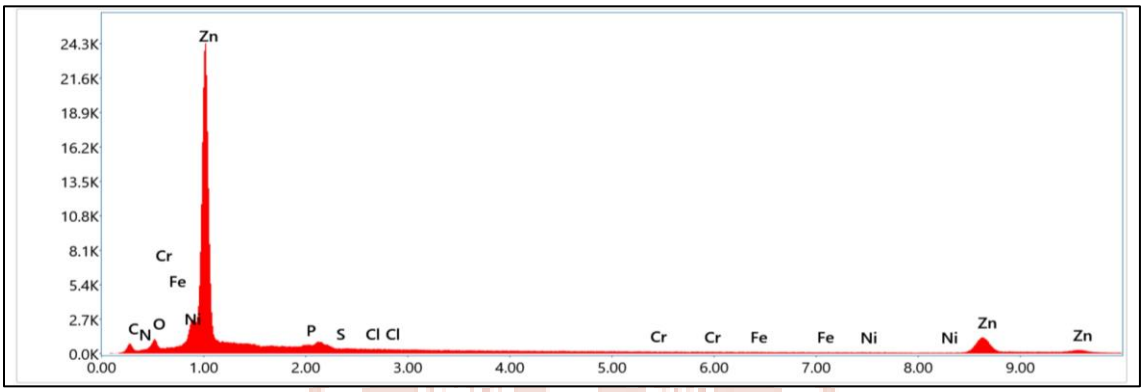

Fig. 8a: EDX images of polished zinc surface.

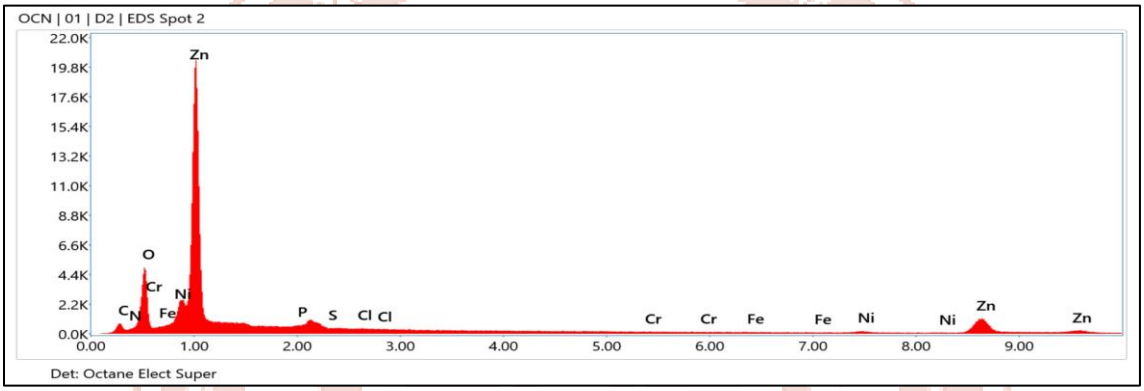

Fig. 8b: EDX images of the zinc surface after 24 h of immersion at 301 ± K in 0.08 N HCl in absence of inhibitor.

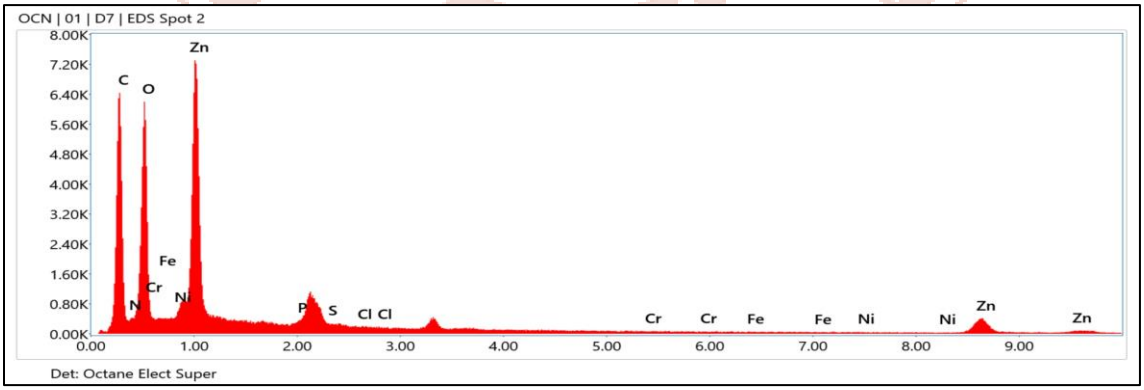

Fig. 8c: EDX images of the zinc surface after 24 h of immersion at 301 ± K in 0.08 N HCl with 2.5 g/L fennel seeds extract.

Table 8: Percentage of different elements composing the zinc surface obtained by EDX spectrum analysis.

System	Percentage (%) of atomic weight of elements									
	%Zn	%C	%N	%O	%P	%S	%Cl	%Cr	%Fe	%Ni
Zn	83.7	11.7	0.0	2.4	1.4	0.6	0.2	0.0	0.0	0.0
Zn + HCl	72.1	8.5	0.0	16.7	0.9	0.6	0.1	0.0	0.0	1.1
Zn + HCl + Fennel seed extract	17.9	54.0	2.2	24.2	0.7	0.7	0.1	0.1	0.1	0.1

The main components in green inhibitors are carbon, nitrogen, and oxygen, which are mostly found in the structures of proteins, amino acids, and alkaloids, as shown in Table 8 mass % of the chemical elements recorded in EDX. On the EDX spectrum of zinc in 0.08 N HCl, Fig. 8b shows the presence of oxygen and chloride peaks with an important amount of zinc and a high percentage of oxygen, indicating that zinc corrosion occurs through a formation of zinc oxide. The EDX spectra of the inhibited sample Fig. 8c showed a high percentage of oxygen and carbon when compared to the blank spectrum, confirming that the inhibitor molecule prevents corrosion by strongly binding to the zinc surface.

3.10 Fourier Transform Infrared Spectroscopy (FTIR):

FTIR spectra are used to identification the functional group and chemical bond present in the compound. Fig. 9c shown the FTIR spectra of the methanolic extraction of fennel seeds. FTIR spectra investigation of fennel seed extract is given Stretching vibration absorption bands at 3277.23 cm^{-1}, 3008.26 cm^{-1}, 2921.34 cm^{-1}, 2851.95 cm^{-1}, 1709.05 cm^{-1}, 1559.53 cm^{-1}, 1457.51 cm^{-1}, 1404.99 cm^{-1}, 1376.65 cm^{-1}, 1249.28 cm^{-1}, 1041.89 cm^{-1}, 991.26 cm^{-1}, 922.84 cm^{-1}, and 718.25 cm^{-1}, which indicates that the C─H, C═C, C═O, C─C, ─OH, C─O─C, and aromatic ring are present in fennel seeds extract. Fig. 9b shows the FTIR spectra of the zinc plate after 24 h of immersion in 200 ml of 0.08 N HCl solution at room temperature (301±1 K) with 2.5 g/L fennel seed extract, giving absorption bands at 3485.33 cm-1, 2917.84 cm-1, 2849.48 cm-1, 1743.26 cm-1, 1536.20 cm-1, 1458.99 cm-1, 1453.62 cm-1, 1397.86 cm-1, 1153.59 cm-1, 1036.92 cm-1, 897.15 cm-1 and 719.67 cm-1 which is close to the fennel seeds extract FTIR spectra that indicate the inhibitor molecule adsorption onto the metal surface.

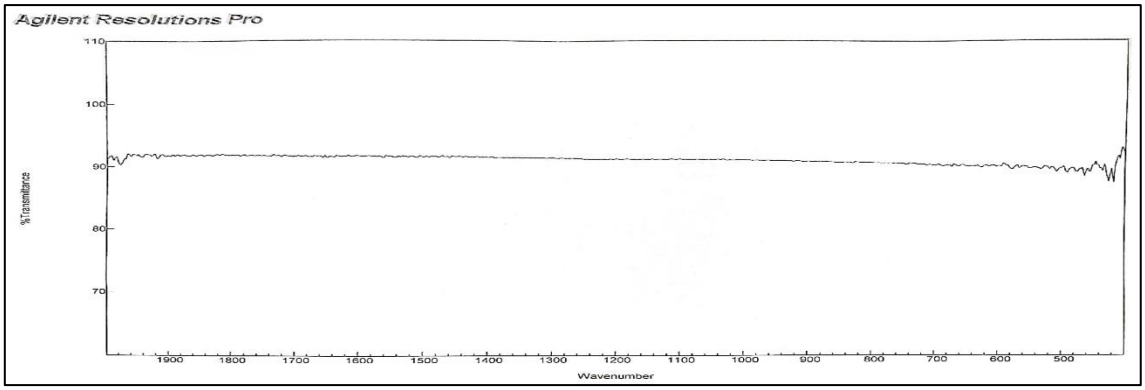

Fig. 9a: IR spectra of the zinc plate after 24 h of immersion at 301 ± K in 0.08 N HCl in absence of inhibitor.

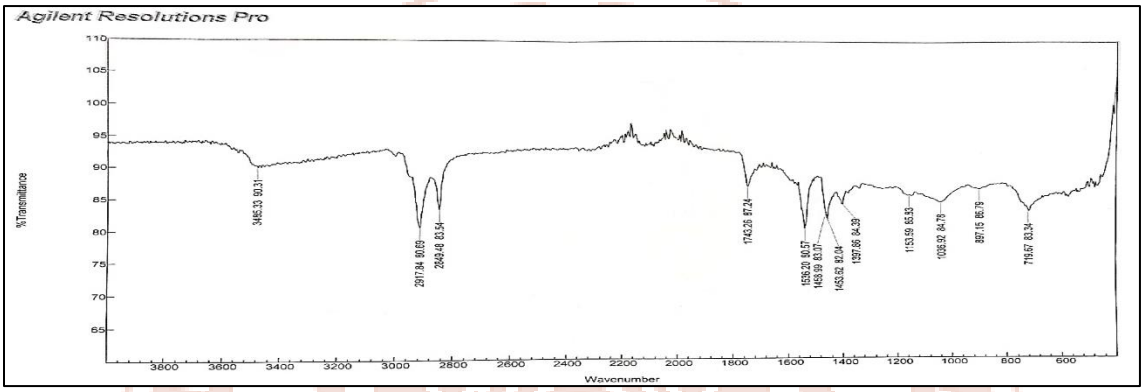

Fig. 9b: IR spectra of the zinc plate after 24 h of immersion at 301 ± K in 0.08 N HCl with 2.5 g/L fennel seeds extract.

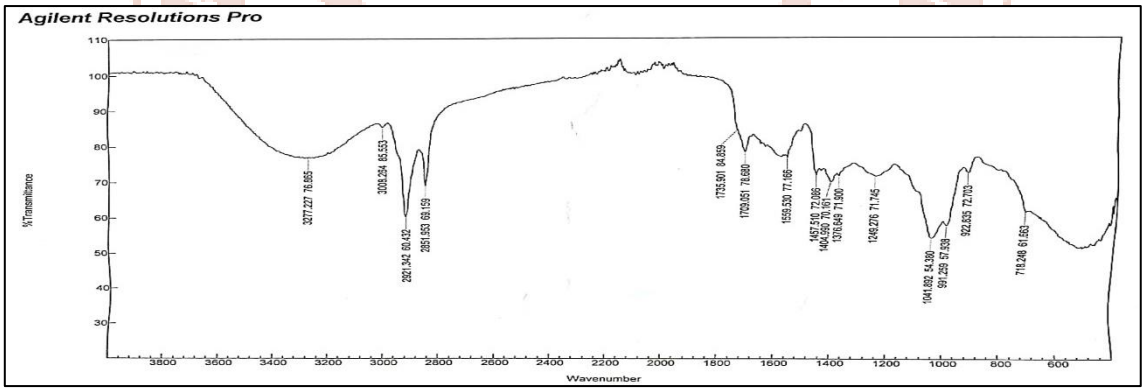

Fig. 9c: IR spectra of the fennel seeds extract.

3.11 Mechanism of corrosion inhibition by fennel seeds extract:

The methanolic extract of fennel seeds showed various phytochemicals such as terpenes, alkaloids, flavonoids, tannins, and saponins. Anethole is the main component in fennel oil. Additional components include camphene, estragole (methyl-chavicol), fenchone, limonene, p-cymene, β-pinene, β-myrcene, β-pinene, bitter fenchone, and safrole [32-33]. The donor-acceptor interaction between the aromatic rings and the pi-electrons of donor oxygen atoms absorption on the metal surface is responsible for the inhibitor molecules adsorbing on the zinc

surface. The -OCH_3 group of anethole and estragole will increase the density of electrons by their inductive or mesomeric effect [34]. Fig. 10 shows the structure of the fundamental components of fennel seeds extract.

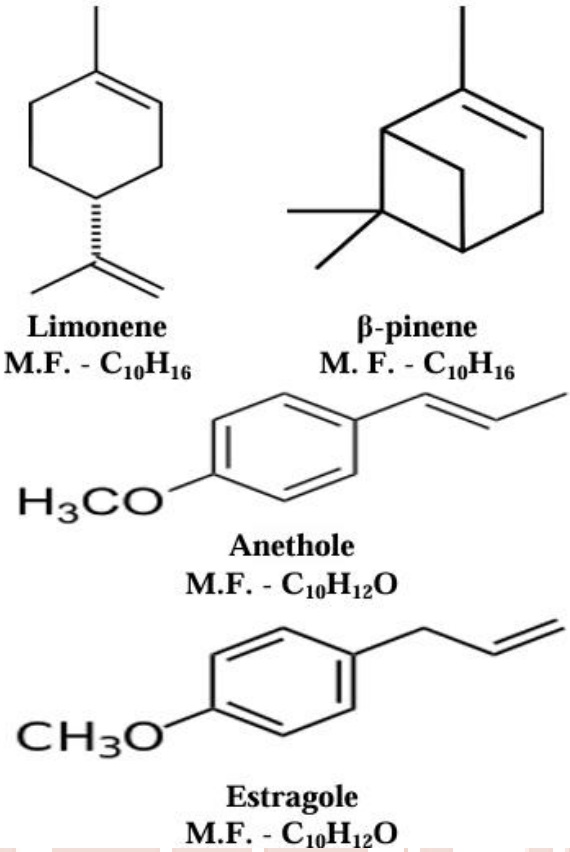

Fig. 10: Structure of main phytoconstituents of fennel seeds extract.

4. Conclusion:

- At the constant acid concentration, the rate of corrosion decreases and inhibition efficiency increases with increases in inhibitor concentrations.
- At the constant inhibitor concentration, the rate of corrosion increases and inhibition efficiency decreases with increases in acid concentrations.
- The graph plot C vs C/θ gives a straight line with nearly a unit slope, indicating that the chemicals' adsorption on the zinc surface follows the Langmuir adsorption isotherm.
- The presence of inhibitors results in the activation energy (E_a) values being higher in inhibited acid, compared to uninhibited acid which suggests that the inhibitors are more effective at lower temperatures.
- The negative values of ΔG_{ads} of inhibitor indicate that the inhibitor molecules' adsorption on the metal surface is a spontaneous exothermic reaction.
- The values of Q_{ads} were negative, suggesting that the adsorption inhibitor molecules on the metal surface.

- All of the inhibitors were given a positive value of enthalpy change (ΔH_{ads}), indicating that the reactions are endothermic and that the corrosion process is supported by higher temperatures.
- The values of entropy change ΔS_{ads} are positive, indicating that the corrosion reaction is entropically favorable.
- SEM shows a smooth surface of inhibited zinc metal compared to the uninhibited system due to the formation of a protective film on the metal.
- EDX shows X-rays for chemical characterization that indicate the peaks related to the green inhibitor's research.
- FTIR spectra confirming that the inhibitor molecule of fennel seeds extract adsorption onto the metal surface.
- The inhibitor efficiency results from mass loss, electrochemical polarization, and electrochemical impedance methods are in good agreement.

Acknowledgement: The authors are thankful to the Department of Chemistry, C. B. Patel Computer College & J. N. M. Patel Science College, Surat for providing laboratory facilities.

Statements & Declarations: The authors declare that no funds, grants, or other support were received during the preparation of this manuscript. The authors declare no conflicts of interest.

References:

1. Pais M., Rao P. (2021), An Up-to-Date Review on industrially significant inhibitors for corrosion control of Zinc, *Journal of Bio- and Tribo-Corrosion*, 7(3). https://doi.org/10.1007/s40735-021-00556-x
2. Desai P. S. (2022), Azadirachita indica (neem) leaf extract used as corrosion inhibitors for mild steel in hydrochloric acid, *Int. J. of Eng. Res.*, 3(1). https://doi.org/10.2139/ssrn.4234427
3. Vashi R. T., Zele S. A., Prajapati N. I. (2022), Inhibitive action of aniline on zinc corrosion in a H_2SO_4 solution: electrochemical study, *Portugaliae Electrochimica Acta*, 40(2), 107-116. https://doi.org/10.4152/pea.2022400205
4. Zele S. A., Patel K. K., Vashi R. T. (2017), Ethanolamines as corrosion inhibitors for zinc in sulphuric acid, *Int. J. of Applicable Chemistry*, 3(3), 350-362.
5. Zele S. A., Vashi R. T., Patel B. B. (2019), Effect of m-Toluidine on The Corrosion Inhibition of Zinc in H_2SO_4, *Int. J. of Res. and Analytical Reviews*, 6(1), 1068-1077.
6. Mahida M. B., Chaudhari H. G. (2012), Aromatic amines as corrosion inhibitors for zinc in hydrochloric acid, *J. of Chemical and Pharmaceutical Research*, 4, 5195-5201.

7. Vashi, R. T., Desai S. A., Desai K. (2019), Diethanolamine as corrosion inhibitor for zinc in hydrochloric acid, *Int. J. of Res. and Analytical Reviews*, 06(1), 490-492.

8. Vashi R. T., Desai K. (2012), Hexamine as corrosion inhibitor for zinc in hydrochloric acid, *Der Pharma Chemica*, 4(5), 2117-2123.

9. Vashi R. T., Desai S.A., Desai P. S. (2008), Ethylamines as Corrosion Inhibitors for Zinc in Nitric Acid, *Asian Journal of Chemistry*, 20(6), 4553-4560.

10. Prabhu R. A., Venkatesha T. V., Praveen B. M. (2012), Electrochemical Study of the Corrosion Behavior of Zinc Surface Treated with a New Organic Chelating Inhibitor, *ISRN Metallurgy*, 1-7. https://doi.org/10.5402/2012/940107

11. Desai P. S., Parmar B. B., Desai F. P., Patel A. M. (2024), Caesalpinia crista (Kanchaki) as green corrosion inhibitor for zinc in hydrochloric acid solutions, *Chemistry Africa*, 7(4), 2173-2187. https://doi.org/10.1007/s42250-023-00874-2

12. Wali, H. F., Bahar S. S. (2021), A study of natural rosmarinus corrosion inhibitor for zinc in HCl solution, *J. of Physics Conference Series*, 1973(1), 012126. https://doi.org/10.1088/1742-6596/1973/1/012126

13. Parmar B., Desai P., Prajapati K. (2024), Bili leaf extract: Green corrosion inhibitor for zinc in hydrochloric acid-experimental and theoretical study, *J. of the Indian Chem. Soc.*, 101(9), 101221. https://doi.org/10.1016/j.jics.2024.101221

14. Dass P. M., Onen A. I., Maitera O. N., Ushahemba G. (2015), Corrosion inhibition of zinc in acid medium by Moringa oleifera and Mangifera indica leaves extracts, *Int. J. of Development and Sustainability*, 9, 940-950. https://www.isdsnet.com/ijds

15. Emembolu L. N., Onukwuli D. O. (2019), Corrosion inhibitive efficacy of natural plant extracts on zinc in 0.5 M HCl solution, *The Pharmaceutical and Chemical Journal*, 6(2)**,** 62-70. https://www.researchgate.net/publication/335107682

16. Abdel-Gaber A., Rahal H., El-Rifai M. (2021), Green Approach towards Corrosion Inhibition in Hydrochloric Acid Solutions, *Biointerface Research in App. Chem.*, 11(6), 14185-14195. https://doi.org/10.33263/briac116.1418514195

17. El-Etre A. Y., Abdallah M., El-Tantawy Z. (2005), Corrosion inhibition of some metals using lawasonia extract, *Corrosion Science*, 47(2), 385.

18. Deyab M. (2014), Egyptian licorice extract as a green corrosion inhibitor for copper in hydrochloric acid solution, *J. of Industrial and Eng. Chem.*, 22:384-389. https://doi.org/10.1016/j.jiec.2014.07.036

19. Chaudhari H. G., Mahida M. M. (2012), Aliphatic amines as corrosion inhibitors for zinc in hydrochloric acid, *Der Pharma Chemica*, 2305-2312. http://derpharmachemica.com/archive.html

20. Langmuir I. (1916), The constitution and fundamental properties of solids and liquids, *Solids Journal of the American Chemical Society*, 38(11), 2221-2295. https://doi.org/10.1021/ja02268a002

21. Onen A. (2014), The behaviour of Moraceae ficus glumosa delile as a corrosion inhibitor for zinc in H_2SO_4, *Chemical Science Review and Letters*, 49-55. http://www.chesci.com/articles/csrl/v3i11S/4_CS21204405

22. Armstrong R., Peggs L. (1994), The behaviour of lead silicate as a corrosion inhibitor for iron and zinc, *Corrosion Science*, 36(5), 749-757. https://doi.org/10.1016/0010-938x(94)90167-8

23. Martinez S., Metikos-Hukovic M. (2003), A nonlinear kinetic model introduced for the corrosion inhibitive properties of some organic inhibitors, *J. of Applied Electrochemistry*, 33(12), 1137-1142. https://doi.org/10.1023/b:jach.0000003851.82985.5e

24. Ansari K. R., Yadav D. K., Ebenso E. E., Quraishi M. A. (2012), Novel and Effective Pyridyl Substituted 1,2,4-Triazole as Corrosion Inhibitor for Mild Steel in Acid Solution, *Int. J. of Electrochemical Science*, 7(5), 4780-4799.

25. Vashi R. T., Desai K. (2012), Hexamine as corrosion inhibitor for zinc in hydrochloric acid, *Der Pharma Chemica*, 4(5), 2117-2123.

26. Ebenso E. E. (2003), Effect of halide ions on the corrosion inhibition of mild steel in H_2SO_4 using methyl red, *Bull. of Electrochemistry*, 19(5), 209-216.

27. Ebenso E. E. (2004), Effect of methyl red and halide ions on the corrosion inhibition of aluminium in H_2SO_4, *Bull. of Electrochemistry*, 20(12), 551-559.

28. Abiola, O. K., Otaigbe J. (2009), The effects of Phyllanthus amarus extract on corrosion and kinetics of corrosion process of aluminum in alkaline solution, *Corrosion Science*, 51(11), 2790-2793. https://doi.org/10.1016/j.corsci.2009.07.006

29. Li W., Zhao X., Liu F., Hou B. (2008), Investigation on inhibition behavior of S-triazole–triazole derivatives in acidic solution, *Corrosion Science*, 50(11), 3261-3266. https://doi.org/10.1016/j.corsci.2008.08.015

30. Desai P., Parmar B., Desai F., Patel A. (2023), Thorn apple (Datura stramonium) extract acts as a sustainable corrosion inhibitor for zinc alloy in hydrochloric acid solutions, *Results in Surfaces and Interfaces*, 14, 100176. https://doi.org/10.1016/j.rsurfi.2023.100176

31. Swetha G., Sachin H. (2021), A study on use of Telmisartan drug for corrosion inhibition of zinc in 0.1M hydrochloric acid: Surface characterization and Quantum studies, *Chemical Data Collections*, 32, 100668. https://doi.org/10.1016/j.cdc.2021.100668

32. Tognolini M., Ballabeni V., Bertoni S., Bruni R., Impicciatore M., Barocelli E. (2007), Protective effect of Foeniculum vulgare essential oil and anethole in an experimental model of thrombosis, *Pharmacological Research*, 56(3), 254-260. https://doi.org/10.1016/j.phrs.2007.07.002

33. Krüger H., Hammer K. (1999), Chemotypes of Fennel (Foeniculum vulgare Mill.), *J. of Essential Oil Research*, 11(1), 79-82. https://doi.org/10.1080/10412905.1999.9701078

34. Al-Saraway A. A., El-Prindary A. A., El Sonbati D.N. (2004), Potentiometric and thermodynamic studies of 3-phenylamino-5-azorhodanine derivatives and their complexes with some transition metals, *Bull. of Electrochemistry*, 20(10), 453-458.